

# Microstructure and microwave dielectric properties of $\text{Li}_2\text{Ti}_{1-x}(\text{Zn}_{1/3}\text{Nb}_{2/3})_x\text{O}_3$ ceramics

Guo-hua Chen<sup>a,b,\*</sup>, Hua-rui Xu<sup>a,b</sup>, Chang-lai Yuan<sup>a,b</sup>

<sup>a</sup>School of Materials Science and Engineering, Guilin University of Electronic Technology, Guilin 541004, China

<sup>b</sup>Guangxi Key Laboratory of Information Materials, Guilin University of Electronic Technology, Guilin 541004, China

Received 31 October 2012; received in revised form 23 November 2012; accepted 23 November 2012

Available online 1 December 2012

## Abstract

$\text{Li}_2\text{Ti}_{1-x}(\text{Zn}_{1/3}\text{Nb}_{2/3})_x\text{O}_3$  ( $0 \leq x \leq 0.5$ ) ceramics were prepared by a solid state ceramic route, and the phase purity, microstructure, and microwave dielectric properties were investigated. The XRD results suggest the formation of solid solutions for all studied compositions ( $0 \leq x \leq 0.5$ ). The dielectric properties are strongly dependent on the compositions, the densifications and the microstructures of the samples. The  $Q \times f$  value increases with  $x$  up to  $x=0.2$  and then decreases with the further increase of  $x$ . The best microwave dielectric properties of  $\epsilon_r=20.5$ ,  $Q \times f=75,257$  GHz, and  $\tau_f=15.4$  ppm/°C could be obtained when  $x=0.2$ .

© 2012 Elsevier Ltd and Techna Group S.r.l. All rights reserved.

**Keywords:** A. Powders-solid state reaction; C. Dielectric properties; Microwave ceramics

## 1. Introduction

With the development of wireless communication, low cost microwave dielectrics with high  $Q$  factor are strongly desired. These microwave dielectric materials must combine a high permittivity ( $\epsilon_r \geq 20$ ), a high unloaded quality factor ( $Q \times f > 40,000$  GHz), and a near zero temperature coefficient of resonant frequency ( $\tau_f$ ) to meet practical applications [1,2]. Dielectric materials subject to these requirements have been reported for microwave and millimeter wave applications and research on new microwave dielectrics is still ongoing and has become a primary issue in the last few years [3–7].

It is well known that Lithium titanium ( $\text{Li}_2\text{TiO}_3$ ), one of the rock-salt type ceramics with a general formula of  $\text{A}_2\text{BO}_3$ , undergoes an order–disorder phase transition at 1213 °C [8]. Moreover, it also possesses a high permittivity ( $\epsilon_r \sim 22.0$ ), a high quality factor ( $Q \times f \sim 63,500$  GHz) and positive  $\tau_f$

value (20.3 ppm/°C) [9]. Bian et al. [10] found that all single rock salt type phase and continuous solid solutions were formed in  $(1-x) \text{Li}_2\text{TiO}_3 + x\text{MgO}$  system ( $0 \leq x \leq 0.5$ ). In addition, the  $(1-x) \text{Li}_2\text{TiO}_3 + x\text{MgO}$  solid solution replacement mechanism could be proposed as  $2\text{Li}^+ + \text{Ti}^{4+} \leftrightarrow 3\text{Mg}^{2+}$ , where charge balance was maintained. The decrease of  $Q \times f$  value at high-level MgO ( $x > 0.3$ ) was owing to the intensity of the (0 0 2) superstructure reflection decreased and became disordered rock-salt structure. When  $x=0.24$ , an excellent combination of microwave dielectric properties ( $\epsilon_r=19.2$ ,  $Q \times f=106,226$  GHz, and  $\tau_f=3.56$  ppm/°C) can be obtained [10]. In general, most ultra-high  $Q$  microwave dielectric ceramics were found in complex perovskites. The high  $Q$  values of the complex perovskites were considered to be related to the high cation ordering degree. More recently, Chen and Zhao [11,12] showed that the  $Q \times f$  value and the  $\tau_f$  can also be improved through the substitution of complex ion  $(\text{Mg}_{1/3}\text{Nb}_{2/3})^{4+}$  for  $\text{Ti}^{4+}$  in  $\text{CaTiO}_3$  and  $\text{Ca}_4\text{La}_2\text{Ti}_5\text{O}_{17}$  system.

In the present work, the  $\text{Li}_2\text{Ti}_{1-x}(\text{Zn}_{1/3}\text{Nb}_{2/3})_x\text{O}_3$  ( $0 \leq x \leq 0.5$ ) ceramics were synthesized to investigate its microwave dielectric properties because the ionic radii of  $(\text{Zn}_{1/3}\text{Nb}_{2/3})^{4+}$  (0.675 Å, CN=6) are similar to that of  $\text{Ti}^{4+}$  (0.605 Å, CN=6) [13]. The resultant microwave

\*Corresponding author at: School of Materials Science and Engineering, Guilin University of Electronic Technology, Guilin 541004, China.  
Tel.: +86 77 3229 1957; fax: +86 77 3229 0129.

E-mail addresses: [cgh1682002@163.com](mailto:cgh1682002@163.com), [chengh@guet.edu.cn](mailto:chengh@guet.edu.cn) (G.-h. Chen).

dielectric property analysis was based on the densification, X-ray diffraction (XRD) patterns, and microstructures of the ceramics. The correction between the microstructure and the  $Q \times f$  value was also investigated.

## 2. Experimental procedure

Samples of  $\text{Li}_2\text{Ti}_{1-x}(\text{Zn}_{1/3}\text{Nb}_{2/3})_x\text{O}_3$  ( $0 \leq x \leq 0.5$ ) were prepared using the conventional solid-state reaction method.  $\text{Li}_2\text{CO}_3$  (+99.5%),  $\text{TiO}_2$  (+99.9%),  $\text{ZnO}$  (+99.9%) and  $\text{Nb}_2\text{O}_5$  (+99.9%) were used as raw materials. Stoichiometric amounts of the raw materials were weighed and wet milled for 24 h using absolute alcohol as lubricant and zirconia balls as milling media, calcined for 2 h at 800 °C, and then remilled with 3 wt% PVA binder. The resultant powders were then uniaxially pressed into cylindrical disks with 12 mm in diameter and 7 mm in thickness under a pressure of 100 MPa. The pellets were preheated at 600 °C for 2 h to remove the organic binder and then sintered for 3 h in air at various temperatures in the range of 1150–1250 °C.

The phase purity of the sintered ceramics was determined using X-ray powder diffraction (XRD) with Cu K $\alpha$  radiation (40 kV and 20 mA, Model D8-Advance, Bruker, Germany). The bulk densities of the sintered ceramics were measured by the Archimedes method. The microstructure of the sintered samples was characterized by scanning electron microscope (SEM) (Model JSM-5610LV, JEOL, Japan). The microwave dielectric properties were obtained using a network analyzer (Model N5230C, Agilent, Santa Clara, CA). The  $\tau_f$  values were measured by noting the variation of resonant frequency of the  $\text{TE}_{011}$  resonant mode over the temperature range of 25 °C–75 °C.

## 3. Results and discussion

X-ray diffraction (XRD) patterns recorded at room temperature from  $\text{Li}_2\text{Ti}_{1-x}(\text{Zn}_{1/3}\text{Nb}_{2/3})_x\text{O}_3$  ( $0 \leq x \leq 0.5$ ) compositions sintered at 1200 °C for 2 h are shown in Fig. 1. All reflections could be adequately indexed according to  $\text{Li}_2\text{TiO}_3$  type (ICDD-PDF: 33–0831) with rock-salt type structure for all specimens, which means that continuous solid solutions are formed. With increasing  $x$  value, the intensity of the (0 0 2) superstructure reflection decreases and become a disordered rock-salt structure at  $x > 0.3$ , suggesting it undergoes an order–disorder phase transition, which is in agreement with that reported previously [10]. It is noted that the diffraction peaks shift to lower angles of  $2\theta$  (for example,  $2\theta \sim 35^\circ$ ,  $37^\circ$  and  $43^\circ$ ) with increasing  $x$  value, which means that the cell volume increases with  $x$  due to the substitution of larger ionic radius of  $(\text{Zn}_{1/3}\text{Nb}_{2/3})^{4+}$  (0.67 Å) for smaller  $\text{Ti}^{4+}$  (0.605 Å). The variation of unit cell volume per oxygen as a function of  $x$  is shown in Fig. 2. The nonlinear increase in unit cell volume from 17.05 Å<sup>3</sup> to 23.82 Å<sup>3</sup> for  $0 \leq x \leq 0.3$  indicates that Vegard's law is not satisfied, which may be attributed to the cations ordering existed in the  $x < 0.4$  samples [14]. Cations ordering generally cause lattice

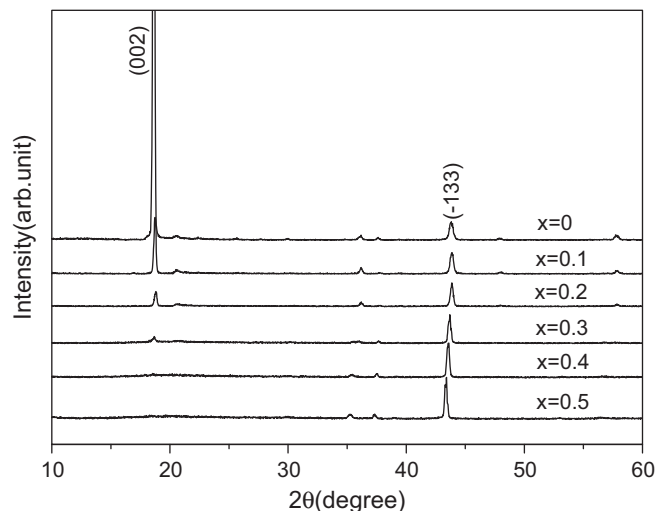


Fig. 1. XRD patterns of  $\text{Li}_2\text{Ti}_{1-x}(\text{Zn}_{1/3}\text{Nb}_{2/3})_x\text{O}_3$  ( $0 \leq x \leq 0.5$ ) ceramics sintered at 1200 °C for 3 h.

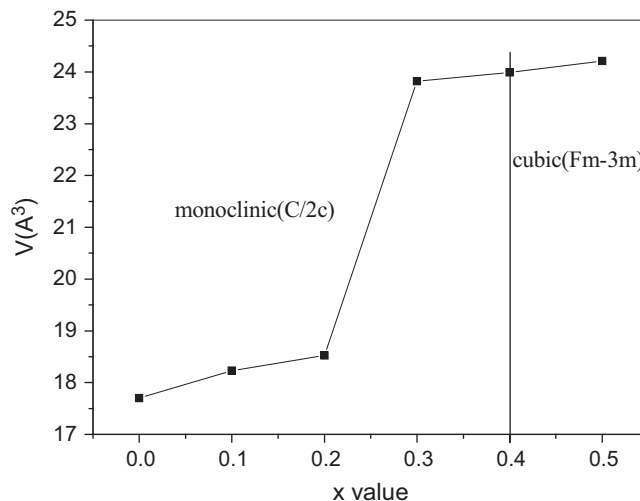


Fig. 2. Variation of unit cell volume per oxygen as a function of  $x$  value in the  $\text{Li}_2\text{Ti}_{1-x}(\text{Zn}_{1/3}\text{Nb}_{2/3})_x\text{O}_3$  ( $0 \leq x \leq 0.5$ ) ceramics.

contraction due to the alleviation of electrostatic repulsion between the like cations by maximizing the cation distance.

Fig. 3 depicts the variation of relative bulk densities as a function of  $x$  value for  $\text{Li}_2\text{Ti}_{1-x}(\text{Zn}_{1/3}\text{Nb}_{2/3})_x\text{O}_3$  ( $0 \leq x \leq 0.5$ ) ceramic samples sintered at different temperatures. For all compositions the relative density increases with sintering temperature and reach maximum density at 1200 °C. Further increasing sintering temperature results in decrease in relative density. With increasing  $x$  value, the relative density first increases and then decrease, and the maximum relative density can be obtained at  $x=0.2$ . Highly densified ceramic samples seem to be difficult to obtain in our experiment. The relative densities for all compositions are lower than 92%, which is probably owing to the evaporation of Li during firing process.

Fig. 4 illustrates the SEM images of samples sintered at 1200 °C with different  $x$  values. The porous microstructure for all samples is observed, which is similar to that of  $\text{Li}_2\text{TiO}_3\text{--MgO}$  systems [10]. The relative uniform surface

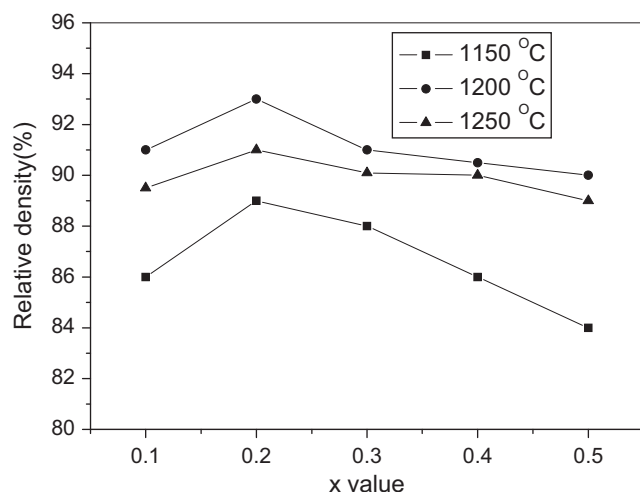


Fig. 3. The variation of relative bulk densities of as a function of  $x$  value for  $\text{Li}_2\text{Ti}_{1-x}(\text{Zn}_{1/3}\text{Nb}_{2/3})_x\text{O}_3$  ( $0 \leq x \leq 0.5$ ) ceramic samples sintered at different temperatures for 3 h.

morphology of the specimens with  $x=0.2$  is observed (Fig. 4b). With increasing  $x$  value, the pores obviously increased. The sample with  $x=0.1$  exhibits a plate like grain structure, and the grain shape changes into regular round polygon when  $x \geq 0.3$ .

Fig. 5 shows the SEM micrographs of the  $\text{Li}_2\text{Ti}_{0.8}(\text{Zn}_{1/3}\text{Nb}_{2/3})_{0.2}\text{O}_3$  ceramic specimens at different temperatures for 2 h. As illustrated, the result indicates that all specimens does not appear dense and the average grain size increases as the sintering temperature increases and varies from 6.6  $\mu\text{m}$  to 25  $\mu\text{m}$  as the temperature increases from 1150 °C to 1250 °C. A uniform surface morphology of the specimens is observed at 1200 °C. However, comparably rapid grain growth is observed at 1250 °C due to the over-sintering of the specimens.

The variation of permittivity as a function of  $x$  value for the  $\text{Li}_2\text{Ti}_{1-x}(\text{Zn}_{1/3}\text{Nb}_{2/3})_x\text{O}_3$  samples sintered at different temperatures is depicted in Fig. 6. The permittivity increases with the sintering temperature or  $x$  value, reaches a maximum, and then starts decreasing, showing a consistent trend with that of density, as shown in Fig. 3. A maximum permittivity ( $\epsilon_r$ ) value of 20.5 is obtained for

$\text{Li}_2\text{Ti}_{0.8}(\text{Zn}_{1/3}\text{Nb}_{2/3})_{0.2}\text{O}_3$  ceramic sample sintered at 1200 °C for 3 h. It is well known that the permittivity is

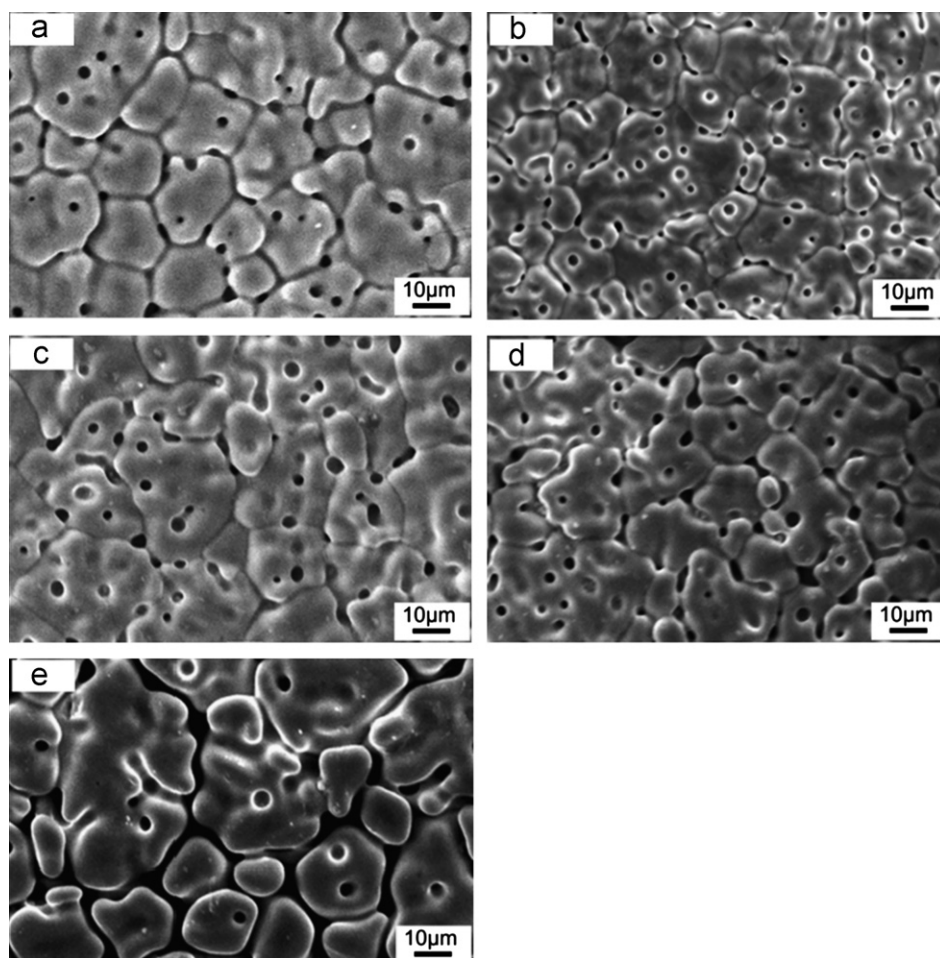


Fig. 4. SEM images of  $\text{Li}_2\text{Ti}_{1-x}(\text{Zn}_{1/3}\text{Nb}_{2/3})_x\text{O}_3$  ceramic samples sintered at 1200 °C for 3 h (a)  $x=0.1$ , (b)  $x=0.2$ , (c)  $x=0.3$ , (d)  $x=0.4$ , (e)  $x=0.5$ .

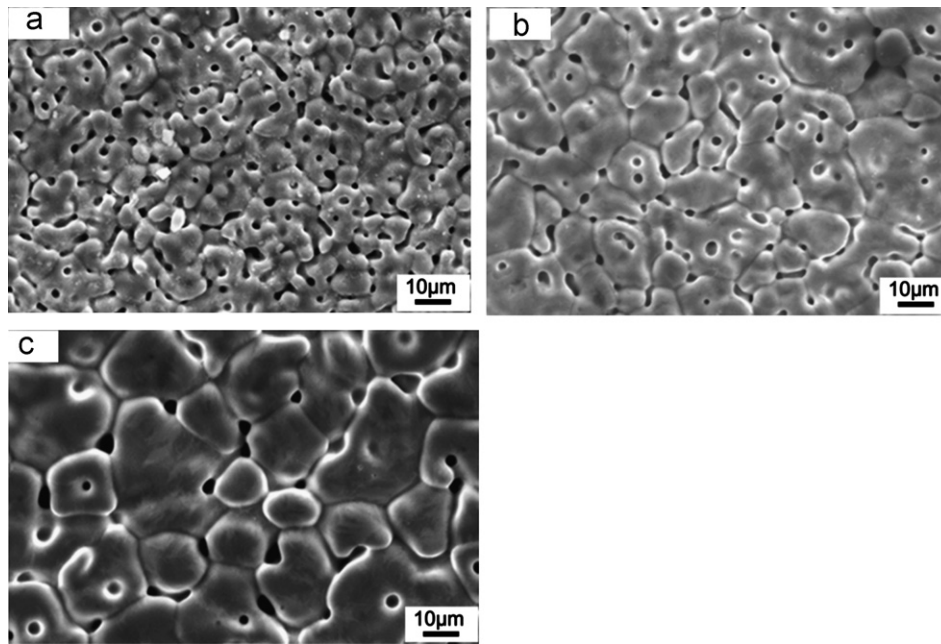


Fig. 5. SEM micrographs of the  $\text{Li}_2\text{Ti}_{0.8}(\text{Zn}_{1/3}\text{Nb}_{2/3})_{0.2}\text{O}_3$  ceramic specimens sintered at (a) 1150, (b) 1200, and (c) 1250 °C for 3 h.

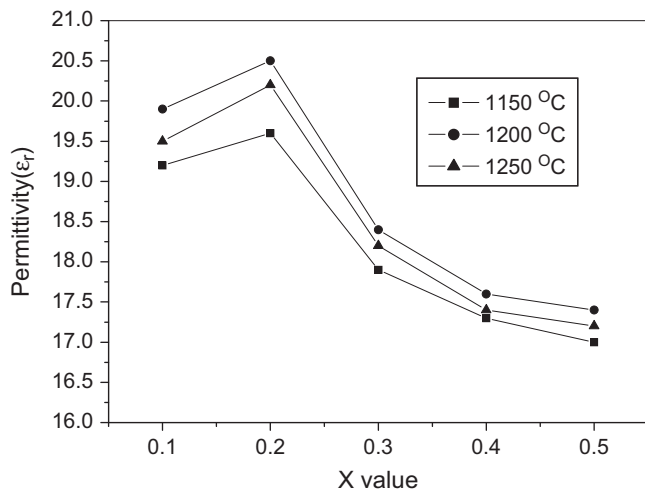


Fig. 6. Variation of permittivity of the  $\text{Li}_2\text{Ti}_{1-x}(\text{Zn}_{1/3}\text{Nb}_{2/3})_x\text{O}_3$  ( $0 \leq x \leq 0.5$ ) ceramic samples sintered at different temperatures for 3 h as a function of  $x$ .

determined by relative density, secondary phase, crystal structure, and lattice defects [15]. The presence of porosity in the sintered ceramics influences the permittivity. Hence, the measured permittivity ( $\epsilon_r$ ) can be corrected ( $\epsilon_{rc}$ ) for the porosity of the ceramics according to Penn's report [16]. Moreover, the permittivity of the microwave dielectric ceramics is known to be affected by average ionic polarizability ( $\alpha_D/V_m$ ) based on the modified Clausius–Mossotti (C–M) equation [17–19]. The molecular volumes, measured permittivity, corrected permittivity, and average ionic polarizability ( $\alpha_D/V_m$ ) of  $\text{Li}_2\text{Ti}_{1-x}(\text{Zn}_{1/3}\text{Nb}_{2/3})_x\text{O}_3$  ( $0 \leq x \leq 0.5$ ) ceramic system sintered at 1200 °C for 3 h are listed in Table 1. It is observed that the measured and

corrected permittivity exhibits same variation trend as a function of  $x$  value. The results (Table 1) suggest that the permittivity is mainly controlled by the porosity and average ionic polarizability ( $\alpha_D/V_m$ ) rather than by the molecular volume ( $V_m$ ) in the  $\text{Li}_2\text{Ti}_{1-x}(\text{Zn}_{1/3}\text{Nb}_{2/3})_x\text{O}_3$  ceramics.

The  $Q \times f$  values of  $\text{Li}_2\text{Ti}_{1-x}(\text{Zn}_{1/3}\text{Nb}_{2/3})_x\text{O}_3$  ( $0 \leq x \leq 0.5$ ) ceramic system sintered at different temperatures for 3 h are demonstrated in Fig. 7. The microwave dielectric loss is caused not only by the lattice vibrational modes but also by the pores, the secondary phases, the lattice defect, or the density [20,21]. By increasing the sintering temperature, the  $Q \times f$  value of the ceramic system is found to increase to a maximum value and decrease thereafter except for pure  $\text{Li}_2\text{TiO}_3$  ( $x=0$ ). It shows a similar trend with that of the relative density because the densification of the ceramics plays an important role in controlling the dielectric loss, and same phenomenon has been shown for other microwave dielectric materials [10]. Moreover, it is found that the  $Q \times f$  values increase with increasing  $x$  up to  $x=0.2$  and then decrease with further increase in  $x$  value. A maximum  $Q \times f$  value of 75,257 GHz could be obtained when  $x=0.2$ . However, the degradation of  $Q \times f$  value at 1250 °C is attributed to the over-sintering resulting in a rapid grain growth leading to a reduction of density as shown in Fig. 3. In addition, at a fixed sintering temperature, the persistent decrease of  $Q \times f$  value when  $x > 0.3$  is owing to the intensity of the (0 0 2) superstructure reflection decreased and a disordered rock-salt structure as well as low densification.

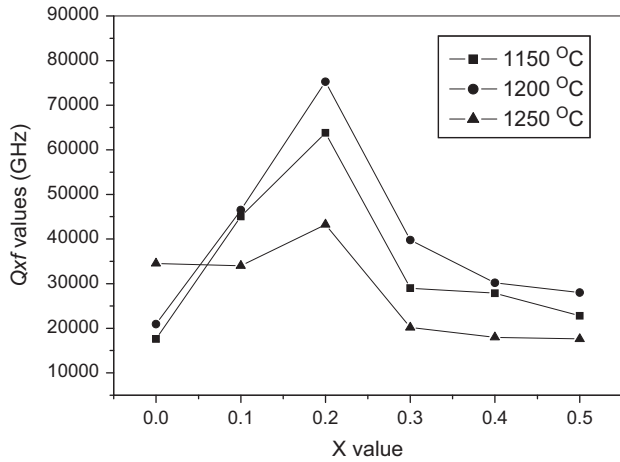
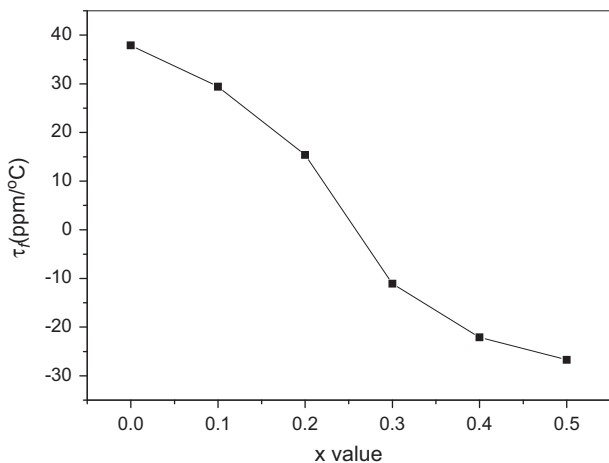
The variation of temperature coefficient of resonant frequency  $\tau_f$  for the samples sintered at 1200 °C for 3 h as a function of  $x$  is shown in Fig. 8. The  $\tau_f$  value decreases monotonically from 37.88 to  $-26.73$  ppm/°C with increasing  $x$ . In the case of perovskite structure compounds, the



Table 1

Molecular volumes ( $V_m$ ), permittivity and average ionic polarizability ( $\alpha_D/V_m$ ) of  $\text{Li}_2\text{Ti}_{1-x}(\text{Zn}_{1/3}\text{Nb}_{2/3})_x\text{O}_3$  ceramics sintered at 1200 °C for 3 h.

$x$ value	Porosity (%)	$V_m$ (Å <sup>3</sup> )	$\epsilon_r$	$\epsilon_{rc}$	$\alpha_D/V_m$	Sintering temperature (°C)
0.0 <sup>a</sup>	6.5	17.85	22.0	24.22	0.2115	1300
0.1	11.0	17.53	19.9	22.96	0.2101	1200
0.2	9.0	17.81	20.5	23.46	0.2108	1200
0.3	11.0	23.82	18.4	21.75	0.2086	1200
0.4	11.5	23.99	17.6	20.96	0.2076	1200
0.5	12.0	24.21	17.4	20.89	0.2074	1200

<sup>a</sup>After Ref. [16].Fig. 7. Variation of  $Q \times f$  values of the  $\text{Li}_2\text{Ti}_{1-x}(\text{Zn}_{1/3}\text{Nb}_{2/3})_x\text{O}_3$  ( $0 \leq x \leq 0.5$ ) ceramics sintered at different temperatures for 3 h as a function of  $x$  value.Fig. 8. Variation of  $\tau_f$  as a function of  $x$  value for the samples sintered at 1200 °C for 3 h.

temperature coefficients of resonant frequency ( $\tau_f$ ) are usually tuned by changing the tilting angle of oxygen octahedrons. In rock-salt structure oxygen octahedrons are edge shared and should not tilt like in perovskites. The value of  $\tau_f$  is related to the temperature coefficient of permittivity ( $\tau_v$ ) and the thermal expansion coefficient ( $\alpha_L$ )

[2,22], as given in the following equation:

$$\tau_f = -\left(\frac{1}{2}\tau_v + \alpha_L\right) \quad (1)$$

where  $\alpha_L$  is the linear thermal expansion coefficient,  $\tau_v$  is the temperature coefficient of dielectric permittivity. In the case of ceramics,  $\tau_f$  is directly influenced by  $\tau_v$  since the magnitude of  $\alpha_L$  is generally constant and insignificant compared to that of  $\tau_v$ . According to Bosman and Colla [23],  $\tau_v$  is composed of three terms:  $A$ ,  $B$ , and  $C$ , as expressed in the following equation:

$$\begin{aligned} \tau_v &= \frac{1}{\epsilon} \left( \frac{\partial \epsilon}{\partial T} \right)_P = \frac{(\epsilon - 1)(\epsilon - 2)}{\epsilon} (A + B + C) \\ A &= \frac{1}{3\alpha_m} \left( \frac{\partial \alpha_m}{\partial T} \right)_V, \quad B = \frac{1}{3\alpha_m} \left( \frac{\partial \alpha_m}{\partial V} \right)_T \times \left( \frac{\partial V}{\partial T} \right)_P \\ C &= \frac{1}{3V} \left( \frac{\partial V}{\partial T} \right)_P \end{aligned} \quad (2)$$

where  $\alpha_m$  and  $V$  denote the polarizability and volume, respectively. The term  $A$  (commonly negative) represents the direct dependence of the polarizability on temperature.  $B$  and  $C$  represent the increase of the polarizability and the decrease of the number of polarizable ions in the unit-cell respectively. The unit cell volume increases with an increase in temperature. The  $B$  and  $C$  terms normally have very similar in magnitude but opposite in sign, therefore the resulting effect on  $\tau_v$  could be generally ignored. Hence, the term  $A$  plays a dominating role. The term  $A$  depends directly on the crystal structures and lattice parameter. In a word, the sign and magnitude of  $\tau_v$  are closely to the dilution of dipoles and increase in dipole strength due to thermal expansion and to the direct dependence on temperature of the polarizabilities. Yoon et al. [24] found that  $\tau_v$  was proportional to the relative magnitude of cell volume in divalent metal tungstate compounds. Fig. 9 shows the relation between temperature coefficient of resonant frequency ( $\tau_f$ ) and unit cell volume. It can be seen that the  $\tau_f$  decreases with increasing unit cell volume, which is in agreement with the results reported by Yoon et al. and Bian et al. [24,10].

#### 4. Conclusions

Microstructure and microwave dielectric properties of  $\text{Li}_2\text{Ti}_{1-x}(\text{Zn}_{1/3}\text{Nb}_{2/3})_x\text{O}_3$  ( $0 \leq x \leq 0.5$ ) system have been

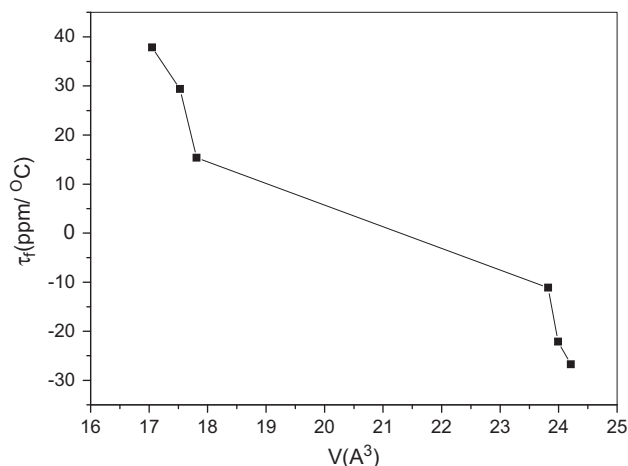


Fig. 9. Variation of  $\tau_f$  as a function of unit cell volume for the samples sintered at 1200 °C for 3 h.

investigated in this paper. XRD results show  $\text{Li}_2\text{Ti}_{1-x}(\text{Zn}_{1/3}\text{Nb}_{2/3})_x\text{O}_3$  is pure phase for the studied compositions ( $0 \leq x \leq 0.5$ ). The ordering degree decreases with increasing  $x$  value. The  $Q \times f$  value is greatly improved by small level substitution of  $(\text{Zn}_{1/3}\text{Nb}_{2/3})$  for Ti ( $x=0.2$ ) due to the uniform microstructure and high densification degree. The permittivity ( $\epsilon_r$ ) is mainly controlled by the porosity and average ionic polarizability ( $\alpha_D/V_m$ ) rather than by the molecular volume ( $V_m$ ) in the  $\text{Li}_2\text{Ti}_{1-x}(\text{Zn}_{1/3}\text{Nb}_{2/3})_x\text{O}_3$  ceramics. Temperature coefficient of resonant frequency ( $\tau_f$ ) decreases monotonically with the increase of  $x$  value. An excellent combined microwave dielectric properties could be obtained when  $x=0.20$ ,  $\epsilon_r=20.5$ ,  $Q \times f = 75,257$  GHz (at  $f=6.6$  GHz), and  $\tau_f = 15.4$  ppm/°C.

## Acknowledgment

This work was supported by the Natural Science Foundation of Guangxi Province, China (2010GXNSFA013029)

## References

- [1] M.T. Sebastian, Dielectric Materials for Wireless Communications, Elsevier Publishers, Oxford, United Kingdom, 2008.
- [2] I.M. Reaney, D. Iddles, Microwave dielectric ceramics for resonators and filters in mobile phone networks, *Journal of the American Ceramic Society* 89 (2006) 2063–2072.
- [3] I.M. Reaney, E.L. Colla, N. Setter, Dielectric and structural characteristics of Ba- and Sr-based complex perovskites as a function of tolerance factor, *Japanese Journal of Applied Physics* 33 (1994) 3984–3990.
- [4] P.L. Wise, I.M. Reaney, W.E. Lee, D.M. Iddles, D.S. Cannell, T.J. Price, Tunability of  $\tau(f)$  in perovskites and related compounds, *Journal of Materials Research* 17 (2002) 2033–2040.
- [5] C.L. Huang, H.L. Chen, C.C. Wu, Improved high  $Q$  value of  $\text{CaTiO}_3\text{--Ca}(\text{Mg}_{1/3}\text{Nb}_{2/3})\text{O}_3$  solid solution with near zero temperature

- coefficient of resonant frequency, *Materials Research Bulletin* 36 (2001) 1645–1652.
- [6] E.A. Nenasheva, L.P. Mudroliubova, N.F. Kartenko, Microwave dielectric properties of ceramics based on  $\text{CaTiO}_3\text{--LnMO}_3$  system (Ln–La, Nd; M–Al, Ga), *Journal of the European Ceramic Society* 23 (2003) 2443–2448.
- [7] K.P. Surendran, M.T. Sebastian, Low loss dielectrics in  $\text{Ba}[(\text{Mg}_{1/3}\text{Ta}_{2/3})_{(1-x)}\text{Ti}_x]\text{O}_3$  and  $\text{Ba}[(\text{Mg}_{1-x}\text{Zn}_x)_{(1/3)}\text{Ta}_{2/3}]\text{O}_3$  systems, *Journal of Materials Research* 20 (2005) 2919–2926.
- [8] M. Castellanos, A.R. West, Order–disorder phenomena in oxides with rock salt structures: the system  $\text{Li}_2\text{TiO}_3\text{--MgO}$ , *Journal of Materials Science* 14 (1979) 450–454.
- [9] J.J. Bian, L. Wang, L.L. Yuan, Microwave dielectric properties of  $\text{Li}_{2+x}\text{Ti}_{1-4x}\text{Nb}_{3x}\text{O}_3$  ( $0 \leq x \leq 0.1$ ), *Materials Science and Engineering: B* 164 (2009) 96–100.
- [10] J.J. Bian, Y.F. Dong, New high Q microwave dielectric ceramics with rock salt structures:  $(1-x)\text{Li}_2\text{TiO}_3 + x\text{MgO}$  system ( $0 \leq x \leq 0.5$ ), *Journal of the European Ceramic Society* 30 (2010) 325–330.
- [11] G.H. Chen, J.C. Di, H.R. Xu, M.H. Jiang, C.L. Yuan, Microwave dielectric properties of  $\text{Ca}_4\text{La}_2\text{Ti}_{5-x}(\text{Mg}_{1/3}\text{Nb}_{2/3})_x\text{O}_{17}$  ceramics, *Journal of the American Ceramic Society* 95 (2012) 1394–1397.
- [12] F. Zhao, Z.X. Yue, Y.C. Zhang, Z.L. Gui, L.T. Li, Microstructure and microwave dielectric properties of  $\text{Ca}[\text{Ti}_{1-x}(\text{Mg}_{1/3}\text{Nb}_{2/3})_x]\text{O}_3$  ceramics, *Journal of the European Ceramic Society* 25 (2005) 3347–3352.
- [13] R.D. Shannon, Revised effective ionic radii and systematic studies of interatomic distances in halides and chalcogenides, *Acta Crystallographica* 32 (1976) 751–767.
- [14] B.M. Castellanos, A.R. West, Deviation from Vegard's law in oxide solid solutions—the system  $\text{Li}_2\text{TiO}_3\text{--Na}_2\text{TiO}_3$ , *Journal of the Chemical Society* 76 (1980) 2159–2169.
- [15] H. Zhou, X. Chen, L. Fang, C. Hu, Preparation and characterization of a new microwave dielectric ceramic  $\text{Ba}_4\text{ZnTi}_{11}\text{O}_{27}$ , *Journal of the American Ceramic Society* 93 (2010) 1537–1539.
- [16] S.J. Penn, N.M. Alford, A. Templeton, X. Wang, M. Xu, M. Reece, Effect of porosity and grain size on the microwave dielectric properties of sintered alumina, *Journal of the American Ceramic Society* 80 (1997) 1885–1888.
- [17] H. Ogawa, A. Kan, S. Ishihara, Y. Higashida, Crystal structure of corundum type  $\text{Mg}_4(\text{Nb}_{2-x}\text{Ta}_x)\text{O}_9$  microwave dielectric ceramics with low dielectric loss, *Journal of the European Ceramic Society* 23 (2003) 2485–2488.
- [18] W. Lei, W.Z. Lu, D. Liu, J.H. Zhu, Phase evolution and microwave dielectric properties of  $(1-x)\text{ZnAl}_2\text{O}_4\text{--}x\text{Mg}_2\text{TiO}_4$  ceramics, *Journal of the American Ceramic Society* 92 (2009) 105–109.
- [19] R.D. Shannon, Dielectric polarizabilities of ions in oxides and fluorides, *Journal of Applied Physics* 73 (1993) 348–366.
- [20] B.D. Silverman, Microwave absorption in cubic strontium titanate, *Physical Review* 125 (1962) 1921–1930.
- [21] H. Tamura, Microwave dielectric losses caused by lattice defects, *Journal of the European Ceramic Society* 26 (2006) 1775–1780.
- [22] P.J. Harrop, Temperature coefficients of capacitance of solids, *Journal of Materials Science* 4 (1969) 370–375.
- [23] J. Bosman A, E.E. Havinga, Temperature dependence of dielectric constants of cubic ionic compounds, *Physical Review* 129 (1963) 1593–1600.
- [24] S.H. Yoon, D.W. Kim, S.Y. Cho, K.S. Hong, Investigation of the relations between structure and microwave dielectric properties of divalent metal tungstate compounds, *Journal of the European Ceramic Society* 26 (2006) 2051–2054.